Modeling IEEE 802.15.4 Networks over Fading Channels

Piergiuseppe Di Marco†, Carlo Fischione†,
Fortunato Santucci‡, and Karl Henrik Johansson†

Abstract

Energy-efficient and flexible communication protocols are instrumental for effective and pervasive development of control and monitoring applications over wireless networks. The IEEE 802.15.4 protocol stack is the de-facto reference communication standard for industrial and home automation. Although the performance of the medium access control (MAC) of this protocol has been thoroughly investigated under the assumption of ideal wireless channel, there is still a lack of understanding of the cross-layer dynamics between MAC and physical layer in the presence of realistic wireless channel models that include path loss, multi-path fading and shadowing. An investigation of these mutual effects is instrumental for consistent performance prediction, correct design and optimization of the protocols in the prospected application scenarios. In this paper, a novel approach to analytical modeling of these interactions and performance prediction is proposed. The analysis considers simultaneously a composite channel fading, interference generated by multiple terminals, the effects induced by hidden terminals, and the MAC reduced carrier sensing capabilities. New results on the MAC-physical layer interactions are derived and validated for single-hop and multi-hop topologies. It is shown that performance indicators of the MAC over fading channels are often far from those derived under ideal channel assumptions. Moreover, it is established to what extent fading may be beneficial for the overall network performance and how the results presented in this paper can be used to drive joint optimization of physical layer and MAC layer parameters.

† ACCESS Linnaeus Center, Electrical Engineering, Royal Institute of Technology, Stockholm, Sweden. E-mail: {pidm|carlofi|kallej}@ee.kth.se. ‡ Centre of Excellence DEWS and Dept. DISIM, University of L'Aquila, L'Aquila, Italy. E-mail: fortunato.santucci@univaq.it. The authors acknowledge the support of the Swedish Foundation for Strategic Research, the Swedish Research Council, the Swedish Governmental Agency for Innovation Systems, and the EU projects Hydrobionets and Hycon2.

Index Terms

IEEE 802.15.4, Medium Access Control, Fading Channel, Interference, Multi-hop topologies, Hidden Terminals, Cross-layer.

I. Introduction

The development of wireless sensor network (WSN) systems relies heavily on understanding the behavior of underlying communication mechanisms. When sensors and actuators are integrated within the physical world with large-scale and dense deployments, potential mobility of nodes, obstructions to propagation, fading of the wireless channel and multi-hop networking must be carefully addressed to offer reliable services. For instance, this is essential for wireless control applications. Indeed, wireless interfaces can represent bottlenecks as they may not provide links as solid as required by applications in terms of guarantees on reliability, delay, and energy efficiency.

There seems to be consensus on that the protocols for physical layer and medium access control (MAC) for low data rate and low power applications in the future will be based on the flexible IEEE 802.15.4 standard with its numerous variants [1]. That standard has been indeed adopted with some modification also by a number of other protocol stacks, including ZigBee, WirelessHART, ISA-100. It is already being used for applications in industrial control, home automation, health care, and smart grids. Nevertheless, there is not yet a clear understanding of the achievable performance of the IEEE 802.15.4 protocol stack, with the consequent inability to adapt the communication performance (e.g., through cross-layer optimization) to meet challenging quality of service constraints.

The IEEE 802.15.4 MAC layer has received much attention, with focus on performance characterization in terms of reliability (i.e., successful packet reception probability), packet delay, throughput, and energy consumption. Some initial works, such as [2], are based on Monte Carlo simulations. More recent investigations have attempted to model the protocol performance by theoretical analysis for single hop networks [3]–[9]. These analytical studies are almost all based on extensions of the Markov chain model originally proposed by Bianchi for the IEEE 802.11 MAC protocol [10]. In [11], modelling of packet losses due to channel fading have been introduced into the homogeneous Markov chain developed for the IEEE 802.15.4 MAC setup

presented in [5]. However, fading is considered only for single packet transmission attempts, the effect of contention and multiple access interference is neglected, and the analysis is neither validated by simulations nor by experiments. In [12], [13], the optimal carrier sensing range is derived to maximize the throughput for IEEE 802.11 networks; however, statistical modeling of wireless fading has not been considered, but a two-ray ground radio propagation model is used in [12] and only the path loss is considered in [13].

The technical contributions surveyed above focus on modeling the typical MAC mechanisms, such as the finite retry limits of the carrier sense multiple access with collision avoidance (CSMA/CA), the carrier sensing range, saturated and unsaturated traffic conditions. However, as already stated, the presence of the wireless channel has been either neglected or only marginally considered. Actually, simulations show that the studies mentioned above may yield highly inaccurate results in terms of reliability, delay, and energy consumption as soon as realistic wireless channel behaviours and interference profiles are introduced. In this regard, recent studies have investigated the performance of multiple access networks in terms of multiple access interference and capture effect [14]. However, in [14] the model of the MAC mechanism is limited to homogeneous single-hop networks (same wireless channel for every node) with uniform random deployment. Moreover, the fading caused by multi-path propagation and shadowing effects have not been considered, while it is known that it may have a crucial impact on the performance of packet access mechanisms [15].

In this paper we propose a novel analytical model that is able to capture the cross-layer interactions of IEEE 802.15.4 MAC and physical layer over interference-limited wireless channels with composite fading models. The main original contributions are as follows:

- We propose a general modeling approach for characterization of the MAC performance with heterogeneous network conditions, a composite Nakagami-lognormal channel, explicit interference behaviours and cross-layer interactions.
- Based on the new model, we determine the impact of fading conditions on the MAC performance under various settings for traffic, inter-node distances, carrier sensing range, and signal-to-(interference plus noise)-ratio (SINR). We show how existing models of the MAC available from the literature may give unsatisfactory or inadequate predictions for performance indicators in fading channels.

- We discuss system configurations in which a certain severity of the fading may be beneficial for overall network performance. Based on the new model, it is then possible to derive optimization guidelines for the overall network performance, by leveraging on the MAC-physical layer interactions.

To determine the network operating point and the performance indicators in terms of reliability, delay, and energy consumption for single-hop and multi-hop topologies, a moment matching approximation for the linear combination of lognormal random variables based on [16] and [17] is adopted in order to build a Markov chain model of the MAC mechanism that embeds the physical layer behavior. In particular, the challenging part of the new analytical setup proposed in this paper is to properly model the rather complex interaction between the MAC protocol and the wireless channel with explicit description of the dependence on several topological parameters and network dynamics. For example, we include failures of the channel sensing mechanism and the presence of hidden terminals, namely nodes that are in the communication range of the destination but cannot be listened by the transmitter. Whether two wireless nodes can communicate with each other depends on their relative distance, the transmission power, the wireless propagation characteristics and interference caused by concurrent transmissions on the same radio channel: the higher the SINR is, the higher the probability that packets can be successfully received. The number of concurrent transmission depends on the traffic and the MAC parameters. In this paper, we describe how to account for statistical fluctuations of the SINR in the Markov chain model of the MAC.

The remainder of the paper is organized as follows. In Section II, we introduce the network model. In Section III, we derive an analytical model of IEEE 802.15.4 MAC over fading channels. In Section IV, reliability, delay, and energy consumption are derived and the results are extended to multi-hop topologies in Section V. The accuracy of the model is evaluated by Monte Carlo simulations in Section VI, along with a detailed analysis of performance indexes with various parameter settings. Section VII concludes the paper and prospects our future work.

II. Network Model

We illustrate the network model by considering the three topologies sketched in Fig. 1. Nevertheless, the analytical results that we derive in this paper are applicable to any fixed topology.

The topology in Fig. 1a) refers to a single-hop (star) network, where node i is deployed at distance $r_{i,0}$ from the root node at the center, and where nodes forward their packets with single-hop communication to the root node. The topology in Fig. 1b) is a multi-hop linear topology, where every node generates and forwards traffic to the root node by multi-hop communication. The distance between two adjacent nodes is denoted as $r_{i,j}$. In Fig. 1c), we illustrate a multi-hop topology with multiple end-devices that generate and forward traffic according to an uplink routing policy to the root node.

Consider node i that is transmitting a packet with transmission power $P_{\mathrm{tx},i}$. We consider an inverse power model of the link gain, and include shadowing and multi-path fading as well. The received power at node j, which is located at a distance $r_{i,j}$, is then expressed as follows

$$P_{\mathrm{rx},i,j} = \frac{c_0 P_{\mathrm{tx},i}}{r_{i,j}^k} f_i \exp(y_i) \,. \tag{1}$$

The constant c_0 represents the power gain at the reference distance 1 m, and it can account for specific propagation environments and parameters, e.g., carrier frequency and antennas. In the operating conditions for IEEE 802.15.4 networks, the inverse of c_0 (i.e., the path loss at the reference distance) is in the range $40-60$ dB [1]. The exponent k is called path loss exponent, and varies according to the propagation environment in the range $2-4$. The factor f_i models the channel fading due to multi-path propagation, which we assume to follow a Nakagami distribution with parameter $\kappa \geq 0.5$ and p.d.f.

$$p_{f_i}(z) = \kappa^\kappa \frac{(z)^{\kappa-1}}{\Gamma(\kappa)} \exp(-\kappa z),$$

where $\Gamma(\kappa)$ is the standard Gamma function $\Gamma(\kappa) = \int_0^\infty \exp(-x) x^{\kappa-1} dx$. We remark here that the Nakagami distribution is quite general and can model fading environment with various degrees of severity. A random lognormal component models the shadowing effects due to obstacles, with $y_i \ \mathcal{N}(0,\sigma_i^2)$. The standard deviation σ_i is called spread factor of the shadowing.

The model we adopt is accurate for IEEE 802.15.4 in a home or urban environment, in which devices may not be in visibility. In the following section, a generalized model of a heterogeneous network using unslotted IEEE 802.15.4 MAC over multi-path fading channels is proposed.

III. IEEE 802.15.4 MAC AND PHY LAYER MODEL

In this section we propose a novel analytical setup to derive the network performance indicators, namely the reliability as probability of successful packet reception, the delay for successfully received packets, and the average node energy consumption. We first consider a single-hop case, and then we generalize the model to the multi-hop case in Section V.

A. Unslotted IEEE 802.15.4 MAC Mechanism

According to the IEEE 802.15.4 MAC, each node can be in one of the following states: (i) idle state, when the node is waiting for the next packet to be generated; (ii) backoff state; (iii) clear channel assessment (CCA) state; (iv) transmission state.

Let a node be in idle state with probability $p_{\text{idle},i}$. The three variables given by the number of backoffs NB, backoff exponent BE, and retransmission attempts RT are initialized: the default initialization is NB=0, BE=m_0, and RT=0. From idle state, a node wakes up with probability q_i, which represents the packet generation probability in each time unit of duration $S_b =$ *aUnitBackoffPeriod*, and moves to the first backoff state, where the node waits for a random number of complete backoff periods in the range $[0, 2^{BE} - 1]$ time units.

When the backoff period counter reaches zero, the node performs the CCA procedure. If the CCA fails due to busy channel, the value of both NB and BE is increased by one. Once BE reaches its maximum value m_b, it remains at the same value until it is reset. If NB exceeds its threshold m, the packet is discarded due to channel access failure. Otherwise the CSMA/CA algorithm generates again a random number of complete backoff periods and repeats the procedure. A node is in CCA state with probability τ_i, and either moves to the next backoff state if the channel is sensed busy with probability α_i, or moves to transmission state with probability $(1 - \alpha_i)$. The node experiences a delay of *aTurnaroundTime* to turn around from listening to transmitting mode.

The reception of the corresponding ACK is interpreted as successful packet transmission. The node moves from the transmission state to idle state with probability $(1-\gamma_{i,j})$. As an alternative, with probability $\gamma_{i,j}$, the packet sent to node j is lost, and the variable RT is increased by one. As long as RT is less than its threshold n, the MAC layer initializes BE=m_0 and starts again the CSMA/CA mechanism to re-access the channel. Otherwise the packet is discarded due to

the retry limit.

B. MAC-Physical Layer Model

In this subsection, we substantially extend the MAC model presented in [18], which was developed under ideal channel conditions, to include the main features of channel impairments and interference.

Assume packets are generated with Poisson distribution at rate λ_l. The probability of generation of a new packet after an idle unit time is then $q_l = 1 - \exp(-\lambda_l/S_b)$. Effects of a limited buffer size can be included in the expression of q_l, by considering the probability that the node queue is not empty after a packet has been successfully sent, after a packet has been discarded due to channel access failure or due to the retry limit (see [18]).

We define the packet successful transmission time L_s and the packet collision time L_c as

$$\begin{aligned} L_s &= L + t_{\text{ack}} + L_{\text{ack}} + IFS\,, \\ L_c &= L + t_{\text{m,ack}}\,, \end{aligned} \tag{2}$$

where L is the total length of a packet including overhead and payload, t_{ack} is ACK waiting time, L_{ack} is the length of ACK frame, *IFS* is the inter-frame spacing, and $t_{\text{m,ack}}$ is the timeout (waiting for the ACK) in the retransmission algorithm, see details in [1].

The expression of the idle state probability $p_{\text{idle},i}$ can be derived from the normalization condition of the Markov chain model in [18], as

$$p_{\text{idle},i} = \begin{cases} \Big[\frac{1}{2}\left(\frac{1-(2\alpha_i)^{m+1}}{1-2\alpha_i}2^{m_0} + \frac{1-\alpha_i^{m+1}}{1-\alpha_i}\right)\frac{1-y_l^{n+1}}{1-y_l} + (L_s(1-\gamma_{i,j}) + L_c\gamma_{i,j})(1-\alpha^{m+1})\frac{1-y_l^{n+1}}{1-y_l} \\ + \frac{1-q_{cf,l}}{q_l}\frac{\alpha_i^{m+1}(1-y_l^{n+1})}{1-y_l} + \frac{1-q_{cr,l}}{q_l}y_l^{n+1} + \frac{1-q_{\text{succ},l}}{q_l}(1-\gamma_{i,j})\frac{(1-\alpha_i^{m+1})(1-y_l^{n+1})}{1-y_l}\Big]^{-1}\,, \\ \quad \text{if } m \leq \bar{m} = m_b - m_0\,, \\ \Big[\frac{1}{2}\left(\frac{1-(2\alpha_i)^{\bar{m}+1}}{1-2\alpha_i}2^{m_0} + \frac{1-\alpha_i^{\bar{m}+1}}{1-\alpha_i} + \ (2^{m_b}+1)\alpha_i^{\bar{m}+1}\frac{1-\alpha_i^{m-\bar{m}}}{1-\alpha_i}\right)\frac{1-y_l^{n+1}}{1-y_l} \\ +(L_s(1-\gamma_{i,j}) + L_c\gamma_{i,j})(1-\alpha^{m+1})\frac{1-y_l^{n+1}}{1-y_l} + \frac{1-q_{cf,l}}{q_l}\frac{\alpha_i^{m+1}(1-y_l^{n+1})}{1-y_l} \\ + \frac{1-q_{cr,l}}{q_l}y_l^{n+1} + \frac{1-q_{\text{succ},l}}{q_l}(1-\gamma_{i,j})\frac{(1-\alpha_i^{m+1})(1-y_l^{n+1})}{1-y_l}\Big]^{-1}\,, \\ \quad \text{otherwise,} \end{cases} \tag{3}$$

where $y_l = \gamma_{i,j}(1-\alpha_i^{m+1})$. The CCA probability τ_i can be derived as

$$\tau_i = \left(\frac{1-\alpha_i^{m+1}}{1-\alpha_i}\right)\left(\frac{1-x_i^{n+1}}{1-x_i}\right) p_{\mathrm{idle},i} \,. \tag{4}$$

The busy channel probability is

$$\alpha_i = \alpha_{\mathrm{pkt},i} + \alpha_{\mathrm{ack},i} \,, \tag{5}$$

where $\alpha_{\mathrm{pkt},i}$ is the probability that node i senses the channel and finds it occupied by an ongoing packet transmission, whereas $\alpha_{\mathrm{ack},i}$ is the probability of finding the channel busy due to ACK transmission. We are now ready to include the effects of fading channel as it follows.

The busy channel probability due to packet transmissions evaluated at node i is the combination of three events:

- at least one other node has accessed the channel within one of the previous L units of time;
- at least one of the nodes that accessed the channel found it idle and started a transmission;
- the total received power at node i is larger than a threshold a, so that an ongoing transmission is detected by node i.

The combinations of all busy channel events yields the busy channel probability that node i senses the channel and finds it occupied by an ongoing packet transmission

$$\alpha_{\mathrm{pkt},i} = L\,\mathcal{H}_i\left(P_i^{\mathrm{det}}\right) \,, \tag{6}$$

where

$$\mathcal{H}_i(\chi) = \sum_{l=0}^{N-2}\sum_{j=1}^{C_{N,l}}\prod_{k=1}^{l+1}\tau_{k_j}\prod_{h=l+2}^{N}(1-\tau_{h_j})\sum_{m=0}^{k-1}\sum_{n=1}^{C_{k,l}}\prod_{q=1}^{m+1}(1-\alpha_{q_n})\,\chi\prod_{r=m+2}^{k}\alpha_{r_n} \,, \tag{7}$$

$$C_{N,l} = \binom{N-1}{l+1} \,,$$

and

$$P_i^{\mathrm{det}} = \Pr\left[\sum_{q=1}^{m+1} P_{\mathrm{rx},q_n,i} > a\right] \tag{8}$$

is the detection probability. The index k accounts for the events of simultaneous accesses to the channel and the index j enumerates the combinations of events in which a number l of channel

accesses are performed in the network simultaneously. Given N nodes in the network, the index k_j refers to the node in the k-th position in the j-th combination of l out of $N-1$ elements (node i is not included). The index q_n accounts for the combinations of events in which one or more nodes find the channel idle simultaneously.

The busy channel probability due to an ACK transmission follows from a similar derivation. An ACK is sent only after a successful packet transmission:

$$\alpha_{\mathrm{ack},i} = L_{\mathrm{ack}} \mathcal{H}_i \left((1-\gamma_{q_n,w}) P_i^{\mathrm{det}} \right) \ , \tag{9}$$

where L_{ack} is the length of the ACK. The index w denotes the destination node of q_n in the expression of $\mathcal{H}_i$. The detection probability P_i^{det} is evaluated with respect to the set of destination nodes. By summing up Eqs. (6) and (9), we compute α_i in Eq. (5).

We next derive an expression for the packet loss probability $\gamma_{i,j}$, namely the probability that a transmitted packet from node i is not correctly detected in reception by node j, by using similar arguments as above. A packet transmission is not detected in reception if there is at least one interfering node that starts the transmission at the same time and the SINR between the received power from the transmitter and the total interfering power plus the noise level N_0 is lower than a threshold b (outage). In the event of no active interferers, which occurs with probability 1-$\mathcal{H}_i(1)$, the packet loss probability is the probability that the signal-to-noise ratio (SNR) between the received power and the noise level is lower than b. Hence,

$$\gamma_{i,j} = \left(1-\mathcal{H}_i(1)\right) P_{i,j}^{\mathrm{fad}} + \mathcal{H}_i\left(P_{i,j}^{\mathrm{out}}\right) + (2\,L-1)\,\mathcal{H}_i\left(\left(1-P_i^{\mathrm{det}}\right) P_{i,j}^{\mathrm{out}}\right) \ , \tag{10}$$

where $P_{i,j}^{\mathrm{fad}}$ is the outage probability due to composite channel fading on the useful link (with no interferers),

$$P_{i,j}^{\mathrm{fad}} = \Pr\left[\frac{P_{\mathrm{rx},i,j}}{N_0} < b\right] \ , \tag{11}$$

and $P_{i,j}^{\mathrm{out}}$ is the outage probability in the presence of interferers (with composite channel fading on every link),

$$P_{i,j}^{\mathrm{out}} = \Pr\left[\frac{P_{\mathrm{rx},i,j}}{\sum_{q=1}^{m+1} P_{\mathrm{rx},q_n,j} + N_0} < b\right] \ . \tag{12}$$

The expressions of the carrier sensing probability τ_l in Eq. (4), the busy channel probability α_i in Eq. (5), the collision probability in Eq. (10), for $l = 1, \ldots, N$, form a system of non-linear equations that can be solved through numerical methods [19].

We next need to derive the detection probability and the outage probabilities in the devised wireless context. With such a goal in mind, we present some useful intermediate results in the following section.

C. Model of Aggregate Multi-path Shadowed Signals

In this section, we approach the problem of computing the sum of multi-path shadowed signals that appear in the detection probability and in the outage probability.

Consider node i performing a CCA and let us focus our attention on the detection probability in transmission $\Pr\left[\sum_{n=1}^{x} P_{\mathrm{rx},n,i} > a\right]$, where x is the current number of active nodes in transmission. By recalling the power channel model in Eq. (1), let us define the random variable

$$Y_i = \ln\left(\sum_{n=1}^{x} A_{i,n} \exp(y_n)\right) ,$$

with

$$A_{i,n} = c_0 \frac{P_{\mathrm{tx},n}}{r_{n,i}^{k}} f_n,$$

and $y_n \sim \mathcal{N}(0, \sigma_n^2)$. Since a closed form expression of the probability distribution function of Y_i does not exist, we resort to a useful approximation instead. In order to characterize Y_i, we apply the Moment Matching Approximation (MMA) method, which approximates the statistics of linear combination of lognormal components with a lognormal random variable, such that $Y_i \sim \mathcal{N}(\eta_{Y_i}, \sigma_{Y_i}^2)$.

According to the MMA method, η_{Y_i} and σ_{Y_i} can be obtained by matching the first two moments of $\exp(Y_i)$ with the first two moments of $\sum_{n=1}^{x} A_{i,n} \exp(y_n)$, i.e.,

$$M_1 \triangleq \exp\left(-\eta_{Y_i} + \frac{1}{2}\sigma_{Y_i}\right) = \sum_{n=1}^{x} E\{A_{i,n}\} \exp\left(\eta_{y_n} + \frac{1}{2}\sigma_{y_n}\right) , \tag{13}$$

$$M_2 \triangleq \exp\left(-2\eta_{Y_i} + 2\sigma_{Y_i}\right) = \sum_{m=1}^{x}\sum_{n=1}^{x} E\{A_{i,m}A_{i,n}\} \exp\left(\eta_{y_m} + \eta_{y_n} + \left(\frac{\sigma_{y_m}^2}{2} + \frac{\sigma_{y_n}^2}{2} + \rho_{y_m,y_n}\sigma_{y_m}\sigma_{y_n}\right)\right). \tag{14}$$

Solving Eqs. (13) and (14) for η_{Y_i} and σ_{Y_i} yields $\eta_{Y_i} = 0.5\ln(M_2) - 2\ln(M_1)$, and $\sigma^2_{Y_i} = \ln(M_2) - 2\ln(M_1)$. It follows that

$$P_i^{\text{det}} = \Pr\left[\sum_{n=1}^{x} P_{\text{rx},n,i} > a\right] = \Pr\left[\exp(Y_i) > a\right] \approx Q\left(\frac{\ln(a) - \eta_{Y_i}}{\sigma_{Y_i}}\right), \tag{15}$$

where

$$Q(z) = \frac{1}{\sqrt{2\pi}}\int_z^{\infty} \exp\left(-\frac{\nu^2}{2}\right) d\nu.$$

Similar derivations follow for the outage probability in reception:

$$\Pr\left[\frac{P_{\text{rx},i,j}}{\sum_{q=1}^{x} P_{\text{rx},q_n,j} + N_0} < b\right] = \Pr\left[f_i\left(\sum_{n=1}^{x} \frac{P_{\text{tx},n} r_{i,j}^k}{P_{\text{tx},i} r_{n,j}^k} f_n \exp(y_n - y_i) + \frac{N_0 r_{i,j}^k}{P_{\text{tx},i}} f_n \exp(-y_i)\right)^{-1} < b\right].$$

Let us now define the random variable

$$\tilde{Y}_{i,j} = -\ln\left(\sum_{n=1}^{x+1} B_{i,j,n}\exp(\tilde{y}_n)\right),$$

where

$$B_{i,j,n} = \begin{cases} \frac{P_{\text{tx},n} r_{i,j}^k}{P_{\text{tx},i} r_{n,j}^k} f_n & \text{for} \quad n = 1, ..., x \\ \frac{N_0 r_{i,j}^k}{P_{\text{tx},i}} f_n & \text{for} \quad n = x+1 \end{cases},$$

and

$$\tilde{y} = \begin{cases} y_n - y_i & \text{for} \quad n = 1, ..., x \\ -y_i & \text{for} \quad n = x+1 \end{cases}.$$

According to the MMA method, we approximate $\tilde{Y}_i \sim \mathcal{N}(\eta_{Y_i}, \sigma^2_{Y_i})$, where $\eta_{\tilde{Y}_{i,j}}$ and $\sigma_{\tilde{Y}_{i,j}}$ can be obtained by matching the first two moments of $\exp(\tilde{Y}_i)$ with the first two moments of $\sum_{n=1}^{N} B_{i,j,n}\exp(\tilde{y}_n)$, i.e.,

$$\tilde{M}_1 \triangleq \exp\left(-\eta_{\tilde{Y}_{i,j}} + \frac{1}{2}\sigma_{\tilde{Y}_{i,j}}\right) = \sum_{n=1}^{x+1} E\{B_{i,j,n}\}\exp\left(\eta_{\tilde{y}_n} + \frac{1}{2}\sigma_{\tilde{y}_n}\right),$$

$$\tilde{M}_2 \triangleq \exp(-2\eta_{\tilde{Y}_{i,j}} + 2\sigma_{\tilde{Y}_{i,j}}) = \sum_{m=1}^{x+1}\sum_{n=1}^{x+1} E\{B_{i,j,m}B_{i,j,n}\}\exp\left(\eta_{\tilde{y}_m} + \eta_{\tilde{y}_n} + \left(\frac{\sigma^2_{\tilde{y}_m}}{2} + \frac{\sigma^2_{\tilde{y}_n}}{2} + \rho_{\tilde{y}_m,\tilde{y}_n}\sigma_{\tilde{y}_m}\sigma_{\tilde{y}_n}\right)\right),$$

which yields $\eta_{\tilde{Y}_{i,j}} = 0.5\ln(\tilde{M}_2) - 2\ln(\tilde{M}_1)$, $\sigma^2_{\tilde{Y}_{i,j}} = \ln(\tilde{M}_2) - 2\ln(\tilde{M}_1)$. Therefore,

$$P^{\mathrm{out}}_{i,j} = \Pr\left[f_i \exp(\tilde{Y}_{i,j}) < b\right] = \int_0^b \int_0^\infty p_f(z|w) p_{\exp(\tilde{Y}_{i,j})}(w) dw\, dz$$
$$= \int_0^b \int_0^\infty p_f(z|w) \frac{1}{\sqrt{2\pi}\sigma_{\tilde{Y}_{i,j}} w} \exp\left(-\frac{(\ln(w) - \eta_{\tilde{Y}_i})^2}{2\sigma^2_{\tilde{Y}_i}}\right) dw\, dz\,. \tag{16}$$

The analysis above holds for a generic weighted composition of lognormal fadings. In the case of lognormal channel model, where only shadow fading components are considered, (i.e., $f_i = 1$), the outage probability becomes

$$P^{\mathrm{out}}_{i,j} = \Pr\left[\exp(\tilde{Y}_{i,j}) < b\right] \approx 1 - Q\left(\frac{\ln(b) - \eta_{\tilde{Y}_{i,j}}}{\sigma_{\tilde{Y}_{i,j}}}\right)\,. \tag{17}$$

For a Nakagami-lognormal channel, the outage probability becomes

$$P^{\mathrm{out}}_{i,j} = \int_0^b \int_0^\infty \kappa^\kappa \frac{(zw)^{\kappa-1}}{\Gamma(\kappa)} \exp(-\kappa z w) \frac{1}{\sqrt{2\pi}\sigma_{\tilde{Y}_{i,j}} w} \exp\left(-\frac{(\ln(w) - \eta_{\tilde{Y}_i})^2}{2\sigma^2_{\tilde{Y}_i}}\right) dw\, dz$$
$$= \int_0^\infty \frac{1}{\sqrt{2\pi}\sigma_{\tilde{Y}_{i,j}} w} \exp\left(-\frac{(\ln(w) - \eta_{\tilde{Y}_i})^2}{2\sigma^2_{\tilde{Y}_i}}\right) \int_0^b \kappa^\kappa \frac{(zw)^{\kappa-1}}{\Gamma(\kappa)} \exp(-\kappa z w) dz\, dw\,.$$

For integer values of m, the integration in z yields

$$P^{\mathrm{out}}_{i,j} = 1 - \int_0^\infty \frac{1}{\sqrt{2\pi}\sigma_{\tilde{Y}_{i,j}} w} \exp\left(-\frac{(\ln(w) - \eta_{\tilde{Y}_i})^2}{2\sigma^2_{\tilde{Y}_i}}\right) \sum_{i=0}^{\kappa-1} \frac{(\kappa\, b\, w)^i}{\Gamma(i+1)} \exp(-\kappa\, b\, w) dw\,.$$

The mean and standard deviation of Y_i and $\tilde{Y}_{i,j}$ can be obtained by inserting the moments of f_i in the moments of $A_{i,n}$ and $B_{i,j,n}$. For Gamma distributed components f_i, we obtain $E\{f_i\} = 1$ and $E\{f_i^2\} = \frac{\kappa+1}{\kappa}$.

We remark here that the evaluation of P^{det}_i, and $P^{\mathrm{out}}_{i,j}$ can be carried out off-line, with respect to the solution of the system of nonlinear equations that need to be solved when deriving τ_l, α_i and $\gamma_{i,j}$. Therefore, the proposed model can be implemented with only a slight increase of complexity with respect to the analytical model of the IEEE 802.15.4 MAC mechanism presented in [18], and the online computation time is not affected significantly.

IV. Performance Indicators

In this section, we investigate three major indicators to analyze the performance of the IEEE 802.15.4 MAC over fading channels. These indicators will also be used to validate the

analytical model we derived in the previous section, by comparing results obtained from the (approximate) model with those obtained by extensive simulation campaigns. The first one is the reliability, evaluated as successful packet reception rate. Then we consider the delay for the successfully received packets as the time interval from the instant the packet is ready to be transmitted, until an ACK for such a packet is received. Eventually, we consider the energy consumption of network nodes.

A. Reliability

For each node of the network, the reliability is based on the probability that packets are discarded at MAC layer. In unslotted CSMA/CA, packets are discarded due to either (i) channel access failure or (ii) retry limits. A channel access failure happens when a packet fails to obtain clear channel within $m+1$ backoff stages. Furthermore, a packet is discarded if the transmission fails due to repeated packet losses after $n+1$ attempts. Therefore, the reliability is

$$R_i = 1 - P_{\mathrm{cf},i} - P_{\mathrm{cr},i}\,. \tag{18}$$

According to the IEEE 802.15.4 MAC mechanism described in Section III-A, the probability that the packet from node i to node j is discarded due to channel access failure can be expressed as

$$P_{\mathrm{cf},i} = \frac{\alpha_i^{m+1}(1-(\gamma_{i,j}(1-\alpha_i^{m+1}))^{n+1})}{1-\gamma_{i,j}(1-\alpha_i^{m+1})}\,,$$

and the probability of a packet discarded due to retry limits is

$$P_{\mathrm{cr},i} = (\gamma_{i,j}(1-\alpha_i^{m+1}))^{n+1}\,.$$

It is worthwhile mentioning that the last expressions link the reliability at the MAC level with the statistical description of wireless channel environment through Eq. (10) and the analysis of Subsection III-C.

B. Delay

We define the delay D_i for successfully delivered packets from node i. If a packet is discarded due to either the limited number of backoff stages m or the finite retry limit n, its delay is not

included into the average delay.

Let $D_{i,h}$ be the delay for node i that sends a packet successfully at the h-th attempt. The expected value of the delay is

$$\mathbb{E}[D_i] = \sum_{h=0}^{n} \Pr[\mathscr{C}_h|\mathscr{C}]\, \mathbb{E}[D_{i,h}]\,, \tag{19}$$

where the event $\mathscr{C}_h$ denotes the occurrence of a successful packet transmission at time $h+1$ given h previous unsuccessful transmissions, whereas the event $\mathscr{C}$ indicates a successful packet transmission within n attempts. Therefore, we can derive

$$\Pr[\mathscr{C}_h|\mathscr{C}] = \frac{\gamma_{i,j}^{j}(1-\alpha_i^{m+1})^{j}}{\sum_{k=0}^{n}\left(\gamma_{i,j}(1-\alpha_i^{m+1})\right)^{k}} = \frac{\left(1-\gamma_{i,j}(1-\alpha_i^{m+1})\right)\gamma_{i,j}^{j}(1-\alpha_i^{m+1})^{j}}{1-\left(\gamma_{i,j}(1-\alpha_i^{m+1})\right)^{n+1}}\,. \tag{20}$$

We recall that $\gamma_{i,j}$ is the collision probability, which we derived in Eq. (10) together with Eqs. (15) and (17), and $1-\alpha_i^{m+1}$ is the probability of successful channel access within the maximum number of m backoff stages, where α_i^{m+1} follows from (5).

The average delay at the h-th attempt is

$$\mathbb{E}[D_{l,h}] = L_s + h\,L_c + \sum_{l=0}^{h}\mathbb{E}[T_l]\,, \tag{21}$$

where T_l is the backoff stage delay, whereas L_s and L_c are the time periods in number of time units for successful packet transmission and collided packet transmission computed in Eq. (2).

Since the backoff time in each stage k is uniformly distributed in $[0, W_k-1]$, where $W_k = 2^{BE}$, the expected total backoff delay is

$$\mathbb{E}[T_h] = T_{sc} + \sum_{r=0}^{m}\Pr[\mathscr{D}_r|\mathscr{D}]\left(r\,T_{sc} + \sum_{k=0}^{r}\frac{W_k-1}{2}\,S_b\right)\,, \tag{22}$$

where T_{sc} is the sensing time in the unslotted mechanism. The event $\mathscr{D}_r$ denotes the occurrence of a busy channel for r consecutive times, and then an idle channel at the $(r+1)$th time. By considering all the possibilities of busy channel during two CCAs, the probability of $\mathscr{D}_r$ is conditioned on the successful sensing event within m attempts $\mathscr{D}$, given that the node senses an idle channel in CCA. It follows that

$$\Pr[\mathscr{D}_r|\mathscr{D}] = \frac{\alpha_i^{r}}{\sum_{k=0}^{m}\alpha_i^{k}} = \frac{\alpha_i^{r}(1-\alpha_i)}{1-\alpha_i^{m+1}}\,. \tag{23}$$

By applying Eqs. (21) – (23) in Eq. (19), the average delay for successfully received packets is computed. Note that the delay is experienced at the MAC level and is hereby linked to the fading channel through the dependency on α_i and $\gamma_{i,j}$ evaluated in the previous section.

C. Energy Consumption

Here we develop the expression of the total energy consumption of node i as the sum of the contributions in backoff, carrier sense, transmission, reception and idle-queue state:

$$E_{\mathrm{tot},i} = E_{b,i} + E_{s,i} + E_{t,i} + E_{r,i} + E_{q,i}\,. \tag{24}$$

In the following, each component of this formula is derived according to the state probabilities in Section III-A. The energy consumption during backoff is

$$E_{b,i} = P_{\mathrm{id}} \frac{\tau_i}{2} \left(\frac{(1-(2\alpha_i)^{m+1})(1-\alpha_i)}{(1-2\alpha_i)(1-\alpha_i^{m+1})} 2^{m_0} + 1 \right),$$

where P_{id} is the average power consumption in idle-listening state, as we assume that the radio is set in idle-listening state during the backoff stages. The energy consumption for carrier sensing is $E_{s,i} = P_{\mathrm{sc}}\tau_i$, where P_{sc} is the average node power consumption in carrier sensing state. The energy consumption during the transmission stage, including ACK reception, is

$$E_{t,i} =(1-\alpha_i)\tau_i(P_t L + P_{\mathrm{id}} + (P_r(1-\gamma_{i,j}) + P_{\mathrm{id}}\gamma_{i,j})L_{\mathrm{ack}})\,,$$

where P_{t} and P_{r} are the average node power consumption in transmission and reception respectively, and we assume $t_{\mathrm{m,ack}} = L_{\mathrm{ack}} + 1$ in backoff time units S_b. In the single-hop case, we assume that the node is in sleeping state with negligible energy consumption during inactivity periods without packet generation. Hence, the energy consumption during the idle-queue state is given by

$$E_{t,i} = P_{\mathrm{s}}\, p_{\mathrm{idle},i}\,,$$

where P_{s} is the average node power consumption in sleeping mode, and $p_{\mathrm{idle},i}$ is the stationary probability of the idle-queue state as derived in Eq. (3).

In the multi-hop case, as we will see in the next section, relay nodes are in idle-listening state also during the inactivity period (because of the duty cycle policy), and an extra cost for

receiving packets and sent ACKs has to be accounted for.

V. Multi-hop Communications

Here we extend the Markov chain model to a general network in which information is forwarded through a multi-hop communication to a sink node.

The model equations derived in Section III-B are solved for each link of the network, by considering that a generic node i forwards aggregate traffic Q_i. The total average aggregated traffic of node i is $Q_i = q_i/S_b$ pkt/s, where q_i is the probability of having a packet to transmit in each time unit and S_b is the duration of the basic time unit in IEEE 802.15.4. The aim of the following analysis is to investigate the total traffic load Q_l, which we associate to the probability q_l in the per-link model equations. To do so, we need to characterize the traffic distribution in the network according to a routing policy.

We define $\lambda = [0, \lambda_1, ..., \lambda_N]$ the vector of node traffic generation rates, where each component is associated to a node. In addition to λ_i, node i has to forward traffic generated by its children nodes. The effect of routing can be described by the routing matrix $\mathbf{M} \in \mathbb{R}^{(N+1)\times(N+1)}$, in which $M_{i,j} = 1$ if node j is the destination of node i, and $M_{i,j} = 0$ otherwise. We assume that the routing matrix is built such that no cycles exists. We define the traffic distribution matrix $\mathbf{T}$ by scaling $\mathbf{M}$ by the probability of successful reception in each link as only successfully received packets are forwarded, i.e.,

$$T_{i,j} = M_{i,j} R_i \,,$$

where R_i is given by Eq. (18).

Therefore, the vector of node traffic generation probabilities $Q = [0, Q_1, \ldots, Q_N]$ is the solution of a system of flow balance equations $Q = Q\,\mathbf{T} + \lambda$. In steady state, we have

$$Q = \lambda \left[\mathbf{I} - \mathbf{T}\right]^{-1} . \tag{25}$$

where $\mathbf{I} \in \mathbb{R}^{(N+1)\times(N+1)}$ is the identity matrix. As routing is acyclic, it is easy to show that $\mathbf{T}$ has spectral radius less than one, therefore the inverse always exists.

Eq. (25) gives the relation between the idle packet generation probability q_i, the routing matrix $\mathbf{M}$, and the performance at MAC layer (through the link reliability R_i). To obtain the multi-

hop network model, we couple Eq. (25) with the expressions for τ_i, α_i and R_i, as obtained by Eqs. (4), (5), and (18).

With respect to single-hop networks, there is an extra energy consumption $E_{x,i}$ due to the packets and ACKs received by relay nodes based on the routing matrix **M**,

$$E_{x,i} = \sum_{n=1}^{N} M_{n,i}(1-\gamma_{n,i})(1-\alpha_n)\tau_n(P_t L + P_{\mathrm{id}} + (P_r(1-\gamma_{n,i}) + P_{\mathrm{id}}\gamma_{n,i})L_{\mathrm{ack}})\,.$$

We validate and exploit these analytical results in the next section.

VI. Performance Evaluations

In this section, we present numerical results for the new model for various settings, network topology, and operations. We report extensive Monte Carlo simulations to validate the accuracy of the approximations that we have introduced in the model. The settings are based on the default specifications of the IEEE 802.15.4 [1]. We perform simulations both for single-hop and multi-hop topologies.

A. Single-hop Topologies

In this set of performance results, we consider a single-hop star topology in Fig. 1a). We let the number of nodes be $N = 7$, the MAC parameters $m_0 = 3$, $m = 4$, $m_b = 7$, $n = 0$, $L = 7$, $L_{\mathrm{ack}} = 2$ and the physical layer parameters $P_{\mathrm{tx},i} = 0$ dBm, and $k = 2$. We validate our model and study the performance of the network by varying the traffic rate $\lambda_i = \lambda$, $i = 1, ..., N$, in the range $0.1-10$ pkt/s, the radius $r_{i,0} = r$, $i = 1, ..., N$, in the range $0.1-10$ m, the spread of the shadow fading $\sigma_i = \sigma$, $i = 1, ..., N$, in the range $0-6$, and the Nakagami parameter κ in the range $1-3$. Moreover, we show results for different values of the carrier sensing threshold $a = -76, 66, 56$ dBm, and outage threshold $b = 6, 10, 14$ dB.

In Fig. 2, we report the average reliability over all links by varying the node traffic rate λ. The results are shown for different values of the spread σ in the absence of multi-path ($f_i = 1$). There is a good matching between the simulations and the analytical model (18). The reliability decreases as the traffic increases. Indeed, an increase of the traffic generates an increase of the contention level at MAC layer. However, we can observe that the impact of shadow fading can be more relevant with respect to variations in the traffic. Therefore, a prediction based only on

Markov chain analysis of the MAC without including the channel behavior, as in the previous literature, is typically inaccurate to capture the performance of IEEE 802.15.4 wireless networks, especially at larger shadowing spreads.

In Fig. 3, the average delay over all links is reported. Also in this case simulation results follow quite well results obtained from the model as given in Eq. (19). An increase of traffic leads to an increase of the average delay due to the larger number of channel contentions and consequently an increase in the number of backoffs. The spread of shadowing components does not impact on the delay significantly, particularly for low traffic, because lost packets due to fading are not accounted for in the delay computation. When the traffic increases, we note that fading is actually beneficial for the delay. In fact, the delay of successfully received packets reduces by increasing σ. This is because the occurrence of a deep fading reduces the probability of successful transmission. However, since this holds for all nodes, the average number of contending nodes for the CCA may reduce, thus reducing the average delay of successfully received packets. It is not possible to capture this network behavior by using separate models of the IEEE 802.15.4 MAC and physical layers as in the previous literature, since this effect depends on a cross-layer interaction.

In Fig. 4, the average power consumption over all links is presented and compared to the analytical expression in Eq. (24). The number of packet transmissions and ACK receptions is the major source of energy expenditure in the network. Therefore, an increase of the traffic leads to an increase of the power consumption, while performance are marginally affected by the spread of the fading. However, the power consumption is slightly reduced when the spread is $\sigma = 6$, due to the smaller number of received ACKs. Note that no power control policy is implemented.

In Fig. 5, the average reliability is reported as a function of the radius r for different values of the spread σ. Again, analytical results, obtained through Eq. (18), are in good agreement with those provided by simulations. For the ideal channel case (i.e., $\sigma = 0$) the size of the network does not affect the reliability in the range $r = 0.1 - 10$ m. For $\sigma = 6$, the performance degrades significantly as the radius increases. An intermediate behavior is obtained for $\sigma = 3$, where the reliability is comparable to the ideal channel case for short links, but it reduces drastically for $r > 1$ m. The effect is the combination of an increase of the outage probability with the radius

(due to the path loss component), and hidden terminals that are not detected by the CCA.

In Fig. 6, we report the average delay by varying the radius r for different values of the spread σ. The shadowing affects the delay positively and the effect is more significant for larger inter-node distances: in this case the average number of contending nodes for the free channel assessment reduces, thus the busy channel probability reduces, which in turn decreases the average delay of successfully received packets.

In Fig. 7, the average power consumption by varying r is presented. We notice a similar behavior as for the delay. The power consumption reduces with the fading and the increasing size of the network. Nodes spend less time in the backoff and channel sensing procedure due to reduced number of contending nodes and the number of ACKs.

Fig. 8 shows the average reliability as a function of the shadowing spread σ. The results are plotted for different values of the carrier sensing threshold a. The reliability decreases when the threshold a become larger. The impact of the variation of the threshold a is maximum for $\sigma = 0$, and the gap reduces when the spread σ increases. In Fig. 9, the average delay is plotted as a function of the spread σ. Depending on the threshold a, the delay shows a different behavior when increasing σ: it increases for $a = -76$ dBm and it decreases for $a = -66$ dBm, and $a = -56$ dBm. As we discussed above, the spread σ may reduce the delay under some circumstances. However, when the threshold is large, the average number of contenders is less influenced by the fading and does not decrease significantly, while the busy channel probability becomes dominant and the number of backoffs increases, so that the delay increases as well. Fig. 10 reports the average power consumption by varying the spread σ. The power consumption reduces by increasing the threshold a as a consequence of the smaller number of ACK transmissions, although a maximum consumption is observed for low values of the spread σ.

In Fig. 11, we plot the average reliability as a function of the spread σ for different values of the outage threshold b. The threshold b does not affect the performance noticeably for $\sigma = 0$, while the gap in the reliability increases with σ. Note that for a high threshold the reliability tends to increase with σ as long as σ is small or moderate, and it decreases for large spreads. In our setup, a maximum in the reliability is obtained for $\sigma \approx 2$.

In Fig. 12, we report the combined effects of shadow fading and multi-path fading on the

reliability. We show the reliability as a function of the spread σ of the shadow fading for different values of the Nakagami parameter κ. We recall that $\kappa = 1$ corresponds to Rayleigh fading. There is a good match between the simulations and the analytical model (18). The effect of the multi-path is a further degradation of the reliability. However, the impact reduces as the Nakagami parameter κ increases and the fading becomes less severe. In fact, for $\kappa \gg 1$, the effect of multi-path becomes negligible. Furthermore, the multi-path fading and the composite channel evidences the presence of the maximum at $\sigma \approx 2$ in the plot of reliability.

B. Multi-hop Linear Topologies

In this set of performance results, we consider the multi-hop linear topology in Fig. 1b). The number of nodes (and hops) is $N = 5$, with the same MAC and physical layer parameters as in the single-hop case. We validate our model and study the performance of the network as a function of the hop distance $r_{i,j}$ in the range $r = 0.1 - 10$ m, and the spread of the shadow fading in the range $\sigma = 0 - 6$. We show results for each hop, and for different values of the carrier sensing threshold $a = -76, 66, 56$ dBm, and outage threshold $b = 6, 10, 14$ dB.

In Fig. 13, the end-to-end reliability is reported from each node to the destination node for different values of the spread σ. The analytical model follows well the simulation results. The end-to-end reliability decreases with the hop number. This effect is more evident in the presence of shadowing. Fig. 14 shows the end-to-end reliability from the farthest node to the destination by varying the distance r between every two adjacent nodes for different values of the spread σ. The reliability is very sensitive to an increase of hop distance. In Fig. 15, we show the end-to-end reliability by varying the spread σ of the shadow fading. Results are shown for different values of the carrier sensing threshold a. In Fig. 16, we plot the end-to-end reliability for different values of b. Similar considerations as for the single-hop case applies here. However, for the linear topology, the reduction of the carrier sensing range from $a = -76$ dBm to $a = -66$ dBm influences less the reliability since hidden nodes are often out of the communication range of the receiver, therefore the channel detection failure may not lead to collisions.

C. Multi-hop Topologies with Multiple End-devices

We consider the multi-hop topology in Fig. 1c). We use the same MAC and physical layer parameters as in the single-hop case. We consider the end-to-end reliability as the routing metric

and study the performance of the network as a function of the traffic $\lambda_i = \lambda$, $i = 1, ..., N$, in the range $0.1 - 10$ pkt/s, the spread of the shadow fading in the range $\sigma = 0 - 6$. Moreover, we show results for different values of the Nakagami parameter $\kappa = 1 - 3$ and threshold $b = 6, 10, 14$ dB.

In Fig. 17, we report the average end-to-end reliability over all the end-devices by varying the node traffic rate. The results are shown for different values of Nakagami parameter κ with the shadowing spread set to $\sigma = 6$. The impact of the Nakagami parameter κ seems more prominent than variation of the traffic. Fig. 18 shows the end-to-end reliability by varying the spread σ for different values of b. Differently with respect to the single-hop and linear topologies, a variation of the outage threshold b has a strong impact on the reliability also for small to moderate shadowing spread. In fact, due to the variable distance between each source-destination pair, the fading and the outage probabilities affect the network noticeably. Nonetheless, this effect is well predicted by the analytical model we have developed.

VII. Conclusions

In this paper, we proposed an integrated cross-layer model of the MAC and physical layers for unslotted IEEE 802.15.4 networks, by considering explicit effects of multi-path shadow fading channels and presence of interferers. We studied the impact of fading statistics on the MAC performance in terms of reliability, delay, and power consumption, by varying traffic rates, inter-nodes distances, carrier sensing range, and SINR threshold. We observed that the severity of the fading and the physical layer thresholds have significant and complex effects on all performance indicator at MAC layer, and the effects are well predicted by the new model. In particular, the fading has a relevant negative impact on the reliability. The effect is more evident as traffic and distance between nodes increase. However, depending on the carrier sensing and SINR thresholds, a fading with small spread can improve the reliability with respect to the ideal case. The delay for successfully received packets and the power consumption are instead positively affected by the fading and the performance can be optimized by opportunely tuning the thresholds.

We believe that the design of future WSN-based systems can greatly benefit from the results presented in this paper. As a future work, a tradeoff between reliability, delay, and power consumption can be exploited by proper tuning of routing, MAC, and physical layer parameters. Various routing metrics can be analyzed, and the model extended to the presence of multiple sinks.

References

[1] *IEEE 802.15.4 Wireless Medium Access Control (MAC) and Physical Layer (PHY) Specifications for Low-Rate Wireless Personal Area Networks (WPANs)*, 2006, http://www.ieee802.org/15/pub/TG4.html.

[2] J. Zheng and M. L. Lee, "Will IEEE 802.15.4 make ubiquitous networking a reality?: A discussion on a potential low power, low bit rate standard," *IEEE Communications Magazine*, vol. 42, no. 6, pp. 140–146, 2004.

[3] J. Mišić, S. Shaf, and V. Mišić, "Performance of a beacon enabled IEEE 802.15.4 cluster with downlink and uplink traffic," *IEEE Transactions Parallel and Distributed Systems*, vol. 17, no. 4, pp. 361–376, 2006.

[4] S. Pollin, M. Ergen, S. C. Ergen, B. Bougard, L. Perre, I. Moerman, A. Bahai, P. Varaiya, and F. Catthoor, "Performance analysis of slotted carrier sense IEEE 802.15.4 medium access layer," *IEEE Transactions on Wireless Communication*, vol. 7, no. 9, pp. 3359–3371, 2008.

[5] P. Park, P. Di Marco, P. Soldati, C. Fischione, and K. H. Johansson, "A generalized Markov chain model for effective analysis of slotted IEEE 802.15.4," in *Proceedings of the 6th IEEE International Conference on Mobile Ad-hoc and Sensor Systems (MASS)*, 2009.

[6] C. Y. Jung, H. Y. Hwang, D. K. Sung, and G. U. Hwang, "Enhanced Markov chain model and throughput analysis of the slotted CSMA/CA for IEEE 802.15.4 under unsaturated traffic conditions," *IEEE Transactions on Vehicular Technology*, vol. 58, no. 1, pp. 473–478, 2009.

[7] C. Buratti, "Performance analysis of IEEE 802.15.4 beacon-enabled mode," *IEEE Transactions on Vehicular Technology*, vol. 59, no. 4, pp. 2031–2045, 2010.

[8] A. Faridi, M. Palattella, A. Lozano, M. Dohler, G. Boggia, L. Grieco, and P. Camarda, "Comprehensive evaluation of the IEEE 802.15.4 MAC layer performance with retransmissions," *IEEE Transactions on Vehicular Technology*, vol. 59, no. 8, pp. 3917–3932, 2010.

[9] P. Park, P. Di Marco, C. Fischione, and K. H. Johansson, "Modeling and optimization of the IEEE 802.15.4 protocol for reliable and timely communications," *IEEE Transactions on Parallel and Distributed Systems*, 2012, DOI 10.1109/TPDS.2012.159.

[10] G. Bianchi, "Performance analysis of the IEEE 802.11 distributed coordination function," *IEEE Journal on Selected Areas in Communications*, vol. 18, no. 3, pp. 535–547, 2000.

[11] M.-H. Zayani, V. Gauthier, and D. Zeghlache, "A joint model for IEEE 802.15.4 physical and medium access control layers," in *IEEE IWCMC*, 2011.

[12] X. Yang and N. Vaidya, "On physical carrier sensing in wireless ad hoc networks," in *Proceedings of the 25th IEEE International Conference on Computer Communications INFOCOM*, 2005.

[13] H. Zhai and Y. Fang, "Physical carrier sensing and spatial reuse in multirate and multihop wireless ad hoc networks," in *Proceedings of the 25th IEEE International Conference on Computer Communications INFOCOM*, 2006.

[14] C. Gezer, C. Buratti, and R. Verdone, "Capture effect in IEEE 802.15.4 networks: Modelling and experimentation," in *IEEE ISWPC*, 2010.

[15] M. Zorzi and F. Borgonovo, "Performance of capture-division packet access with slow shadowing and power control," *IEEE Transactions on Vehicular Technology*, vol. 46, no. 3, pp. 687 –696, 1997.

[16] M. Pratesi, F. Santucci, and F. Graziosi, "Generalized moment matching for the linear combination of lognormal rvs: application to outage analysis in wireless systems," *IEEE Transactions on Wireless Communications*, vol. 5, no. 5, pp. 1122 –1132, 2006.

[17] C. Fischione, F. Graziosi, and F. Santucci, “Approximation for a sum of on-off log-normal processes with wireless applications,” *IEEE Transactions on Communications*, vol. 55, no. 9, pp. 1822 – 1822, 2007.

[18] P. Di Marco, P. Park, C. Fischione, and K. H. Johansson, “Analytical modeling of multi-hop IEEE 802.15.4 networks,” *IEEE Transactions on Vehicular Technology*, 2012, DOI 10.1109/TVT.2012.2201221.

[19] D. P. Bertsekas and J. N. Tsitsiklis, *Parallel and Distributed Computation: Numerical Methods*. Athena Scientific, 1997.

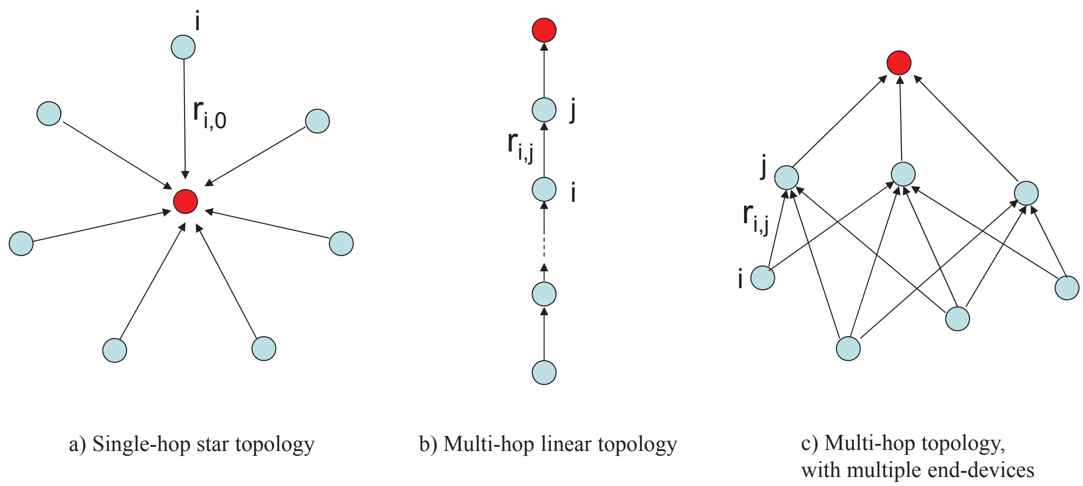

Fig. 1. Example of topologies: single-hop star topology (on the left), multi-hop linear topology (in the center) and multi-hop topology with multiple end-devices (on the right).

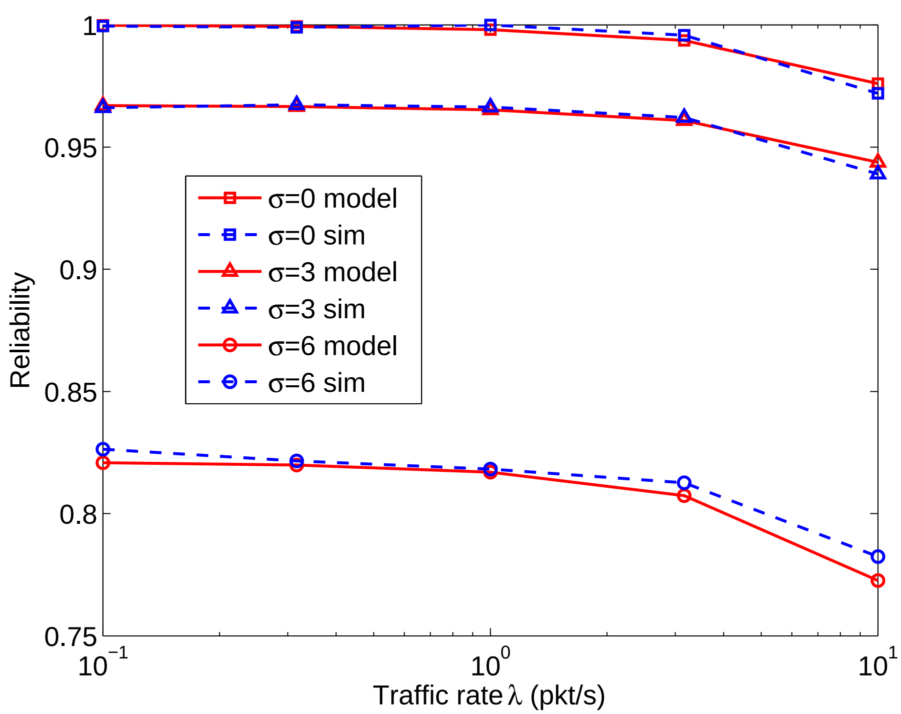

Fig. 2. Reliability vs. traffic rate λ for the star network in Fig. 1a) with $N = 7$ nodes, $r = 1$ m, $a = -76$ dBm, $b = 6$ dB.

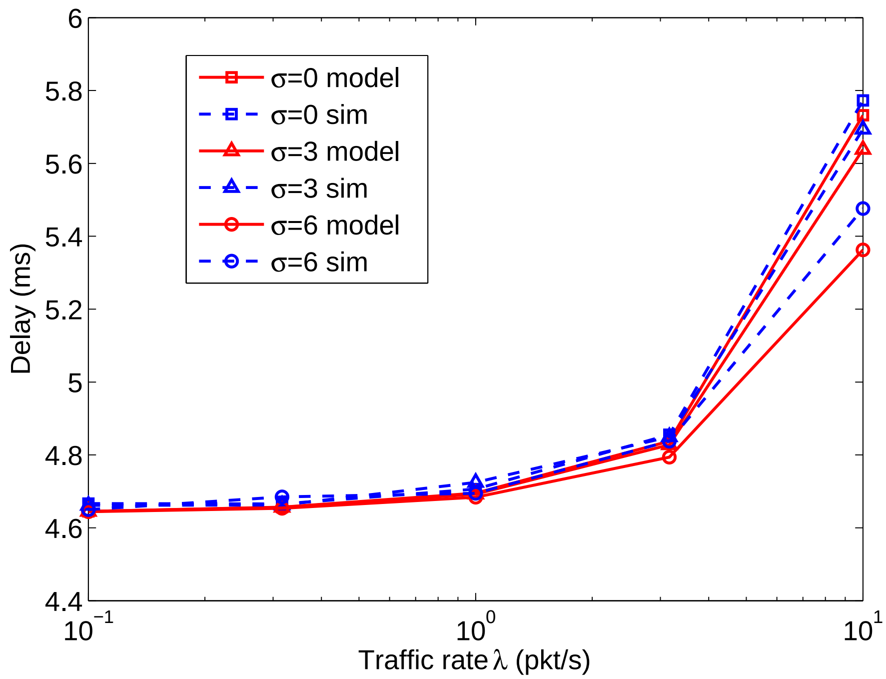

Fig. 3. Delay vs. traffic rate λ for the star network in Fig. 1a) with $N = 7$ nodes, $r = 1$ m, $a = -76$ dBm, $b = 6$ dB.

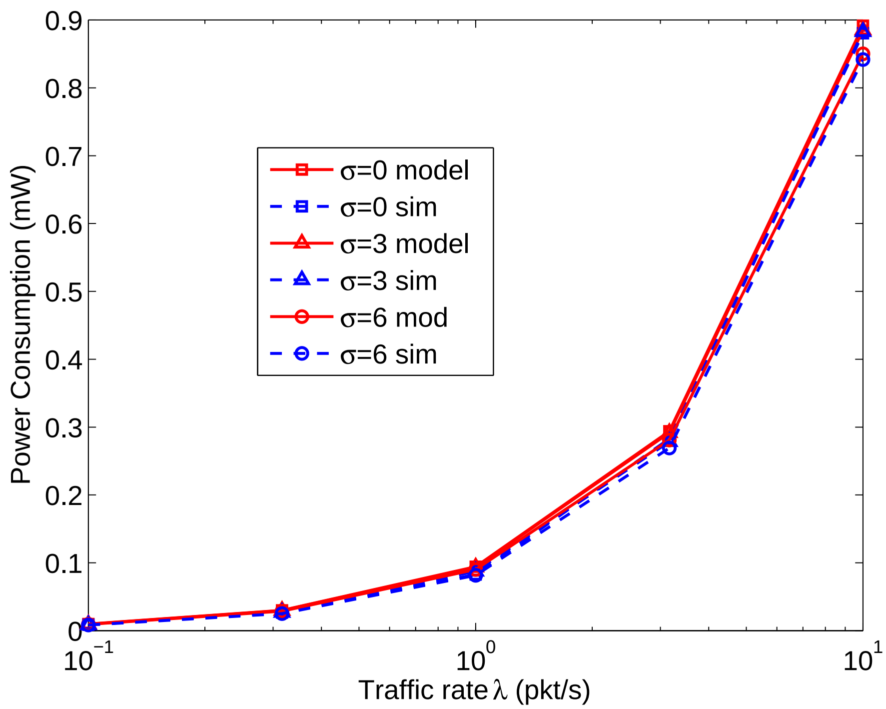

Fig. 4. Power consumption vs. traffic rate λ for the star network in Fig. 1a) with $N = 7$ nodes, $r = 1$ m, $a = -76$ dBm, $b = 6$ dB.

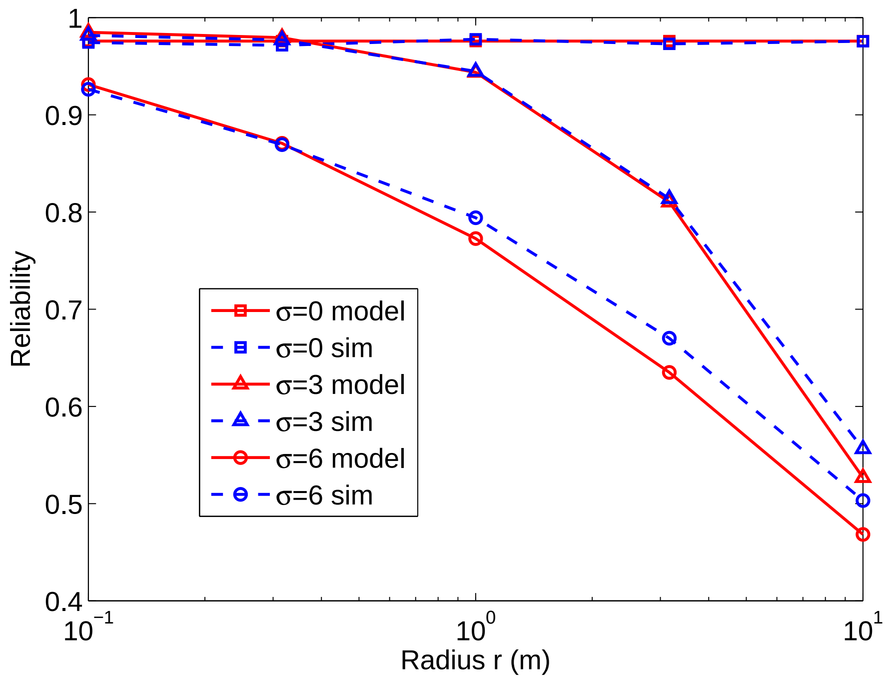

Fig. 5. Reliability vs. radius r for the star network in Fig. 1a) with $N = 7$ nodes, $\lambda = 10$ pkt/s, $a = -76$ dBm, $b = 6$ dB.

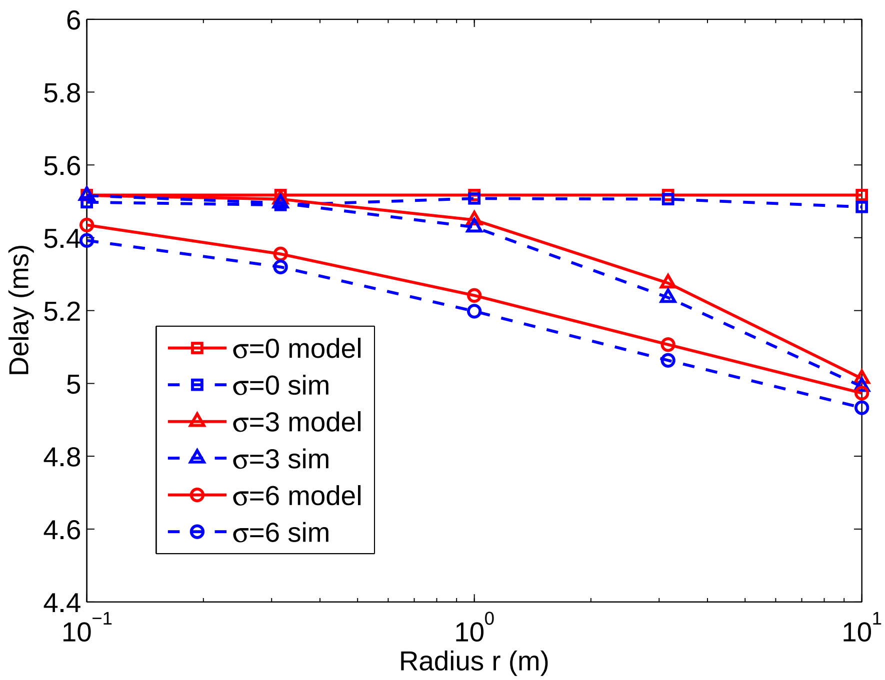

Fig. 6. Delay vs. radius r for the star network in Fig. 1a) with $N = 7$ nodes, $\lambda = 10$ pkt/s, $a = -76$ dBm, $b = 6$ dB.

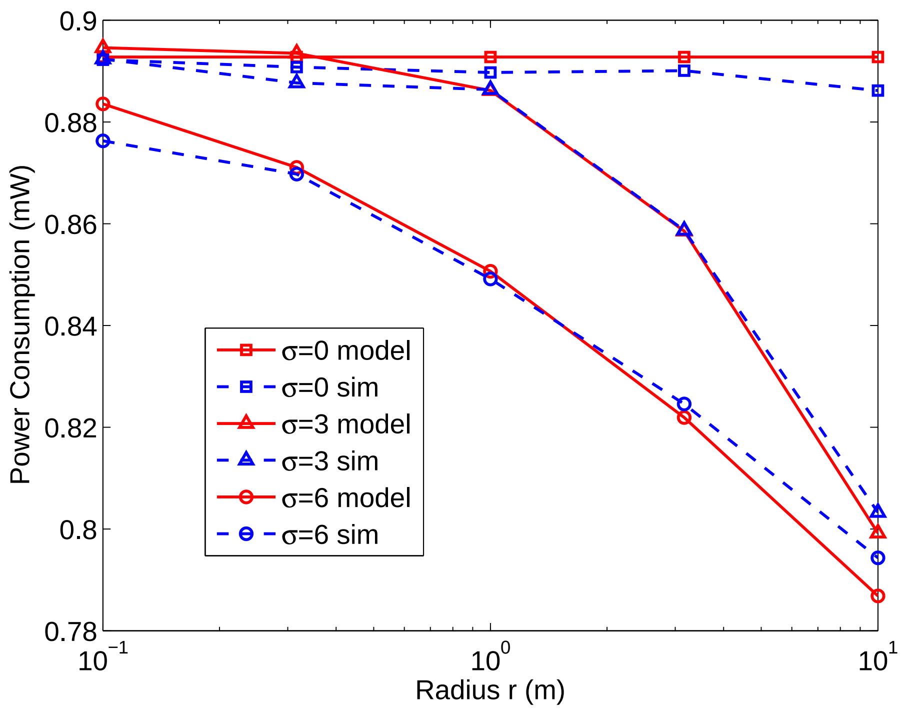

Fig. 7. Power consumption vs. radius r for the star network in Fig. 1a) with $N = 7$ nodes, $\lambda = 10$ pkt/s, $a = -76$ dBm, $b = 6$ dB.

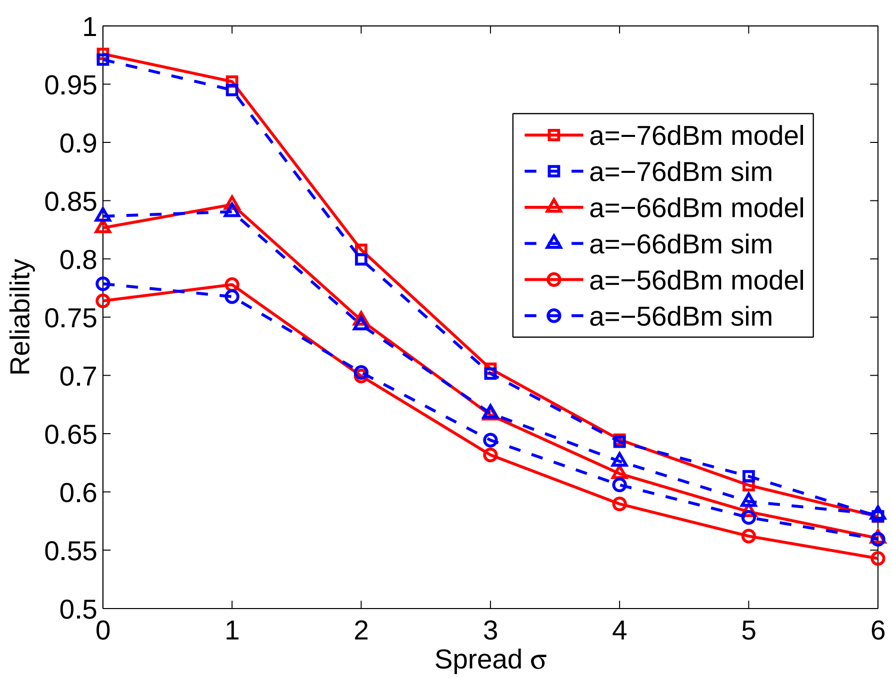

Fig. 8. Reliability vs. σ for the star network in Fig. 1a) with $N = 7$ nodes, $r = 5$ m, $\lambda = 10$ pkt/s, $b = 6$ dB.

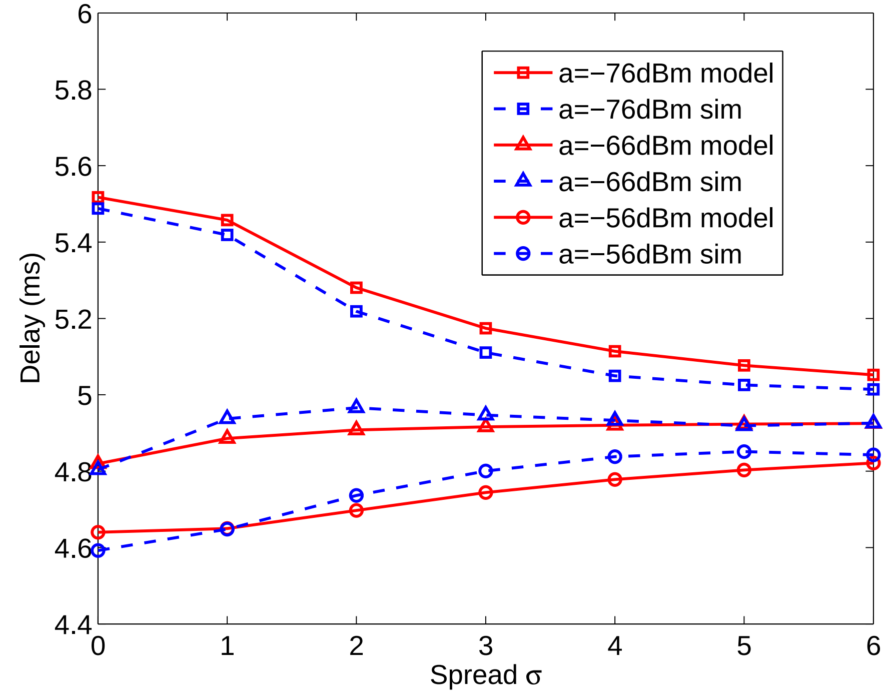

Fig. 9. Delay vs. σ for the star network in Fig. 1a) with $N = 7$ nodes, $r = 5$ m, $\lambda = 10$ pkt/s, $b = 6$ dB.

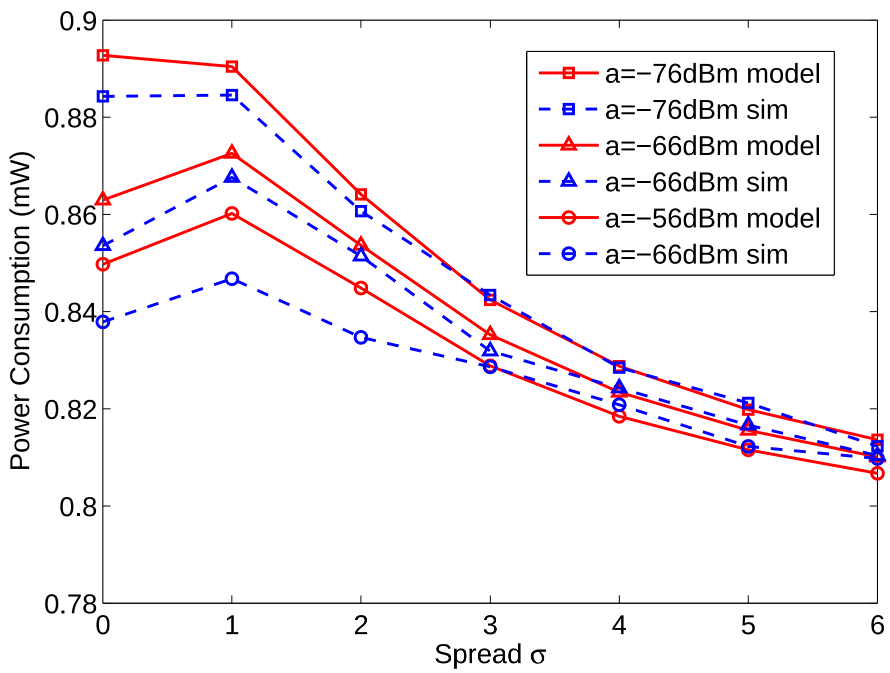

Fig. 10. Power consumption vs. σ for the star network in Fig. 1a) with $N = 7$ nodes, $r = 1$ m, $\lambda = 10$ pkt/s, $b = 6$ dB.

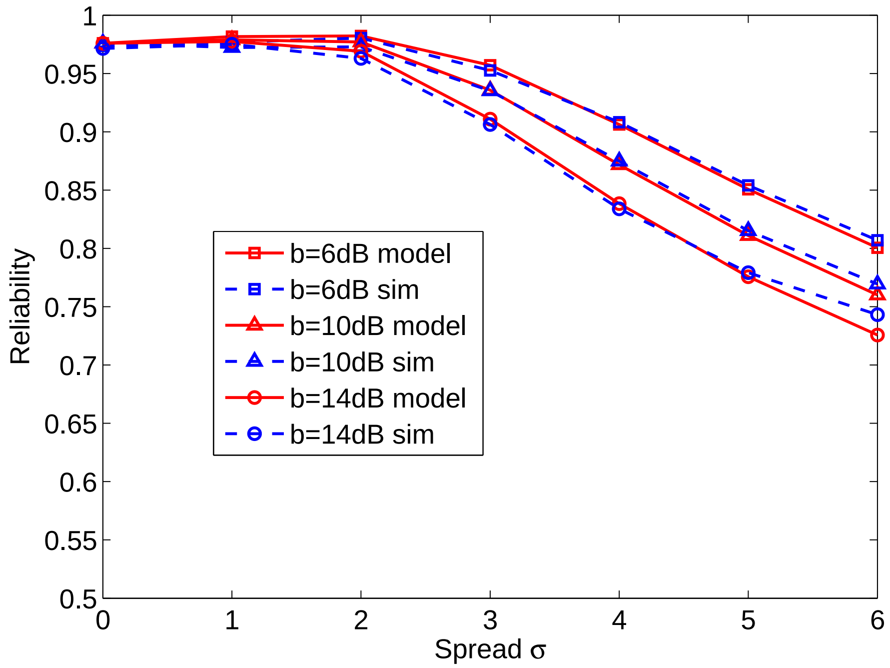

Fig. 11. Reliability vs. σ for the star network in Fig. 1a) with $N = 7$ nodes, $r = 1$ m, $\lambda = 10$ pkt/s, $a = -76$ dB.

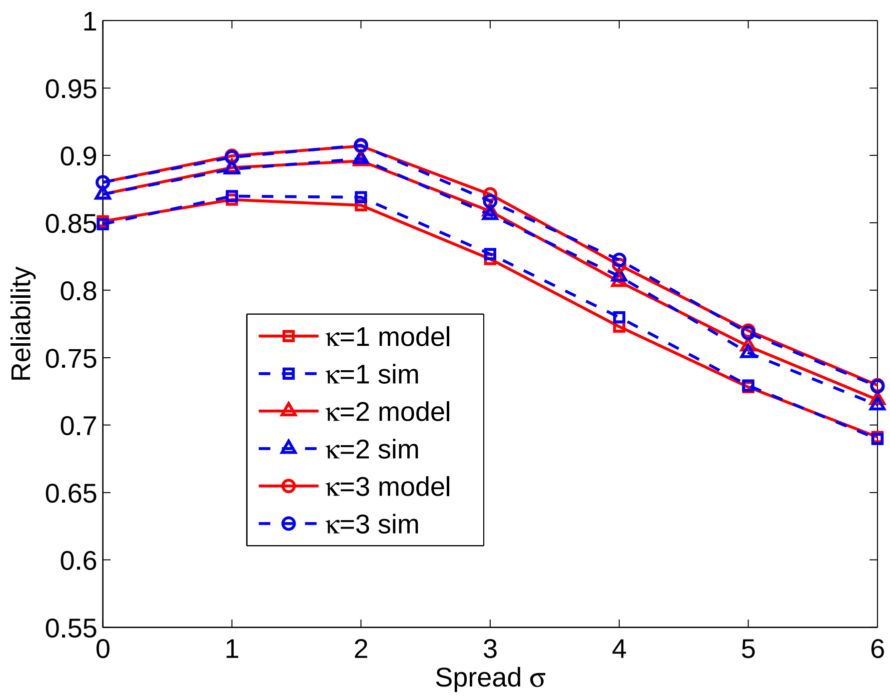

Fig. 12. Reliability vs. σ for the star network in Fig. 1a) with $N = 7$ nodes, $r = 1$ m, $\lambda = 5$ pkt/s, $a = -56$ dB, $b = 6$ dB.

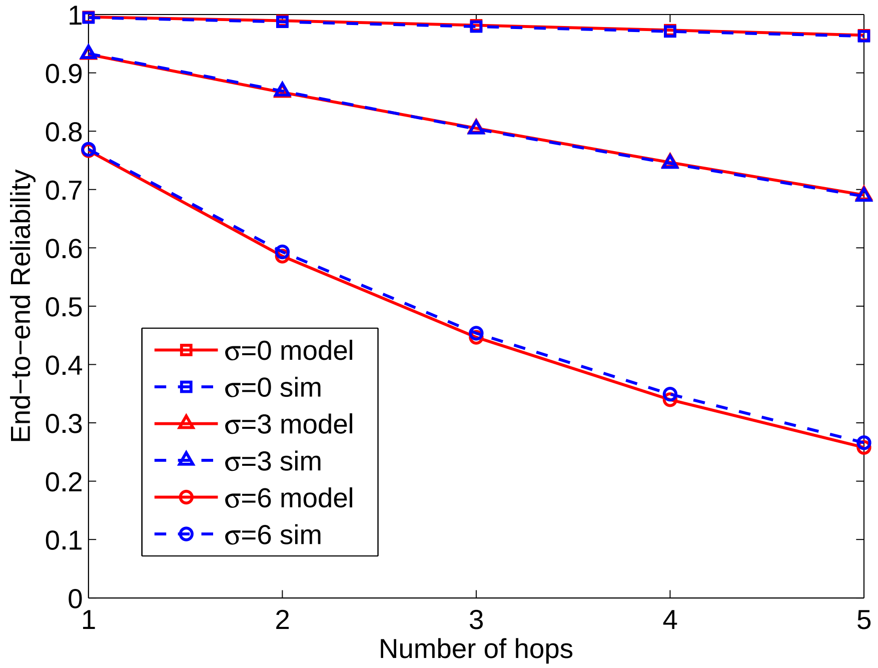

Fig. 13. End-to-end reliability vs. number of hops for the linear topology in Fig. 1b) with $N = 5$ nodes, $r = 1$ m, $\lambda = 2$ pkt/s, $a = -76$ dB, $b = 6$ dB.

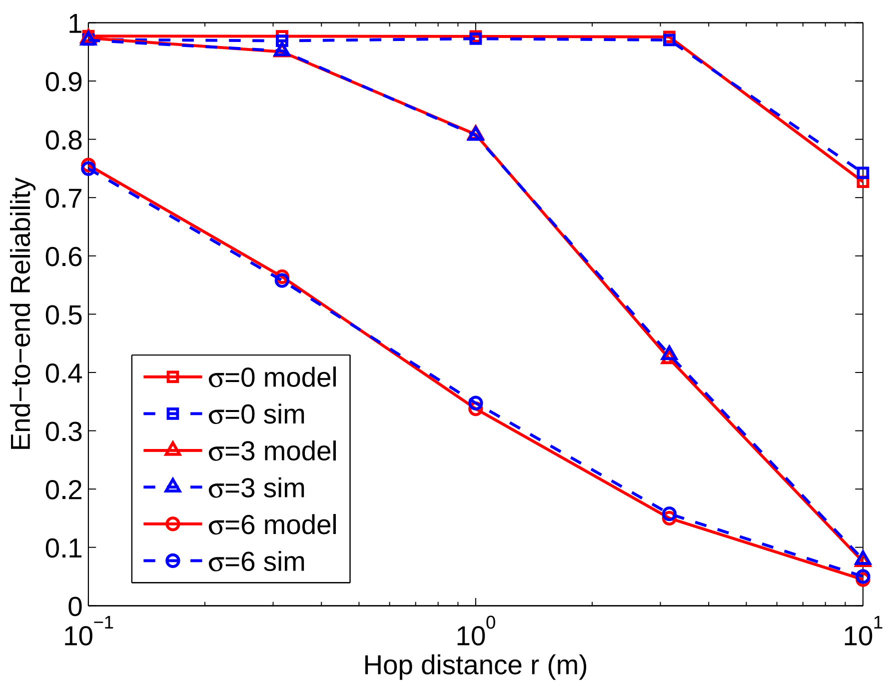

Fig. 14. End-to-end reliability vs. hop distance r for the linear topology in Fig. 1b) with $N = 5$ nodes, $\lambda = 2$ pkt/s, $a = -76$ dB, $b = 6$ dB.

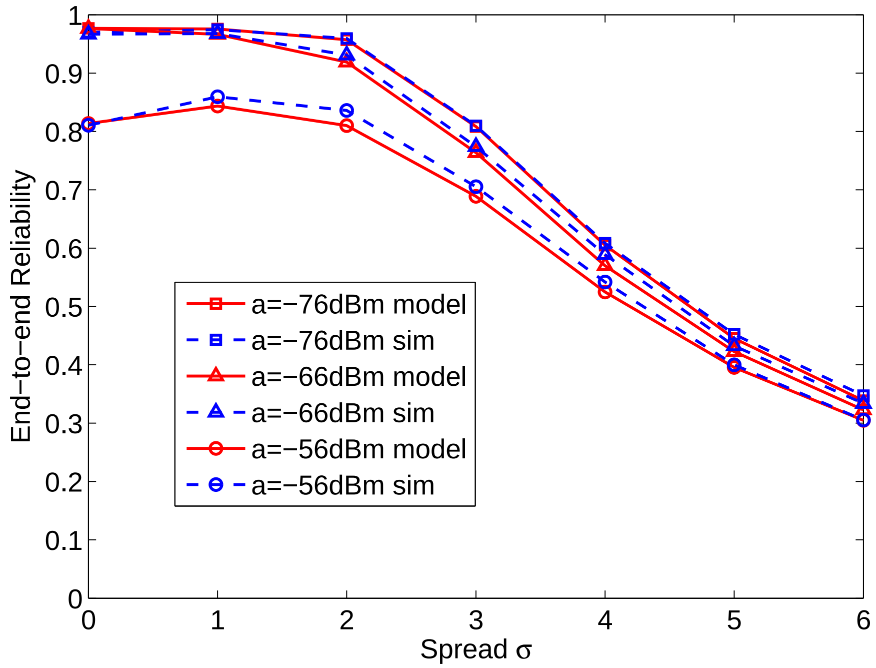

Fig. 15. End-to-end reliability vs. σ for the linear topology in Fig. 1b) with $N = 5$ nodes, $r = 1$ m, $\lambda = 2$ pkt/s, $b = 6$ dB.

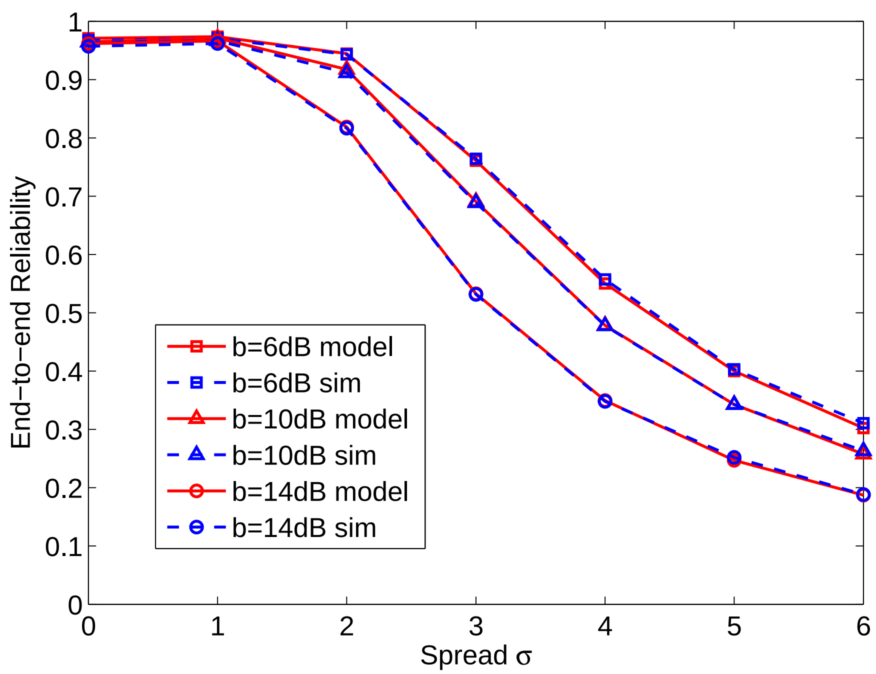

Fig. 16. End-to-end reliability vs. σ for the linear topology in Fig. 1b) with $r = 1$ m, $\lambda = 2$ pkt/s, $a = -76$ dB.

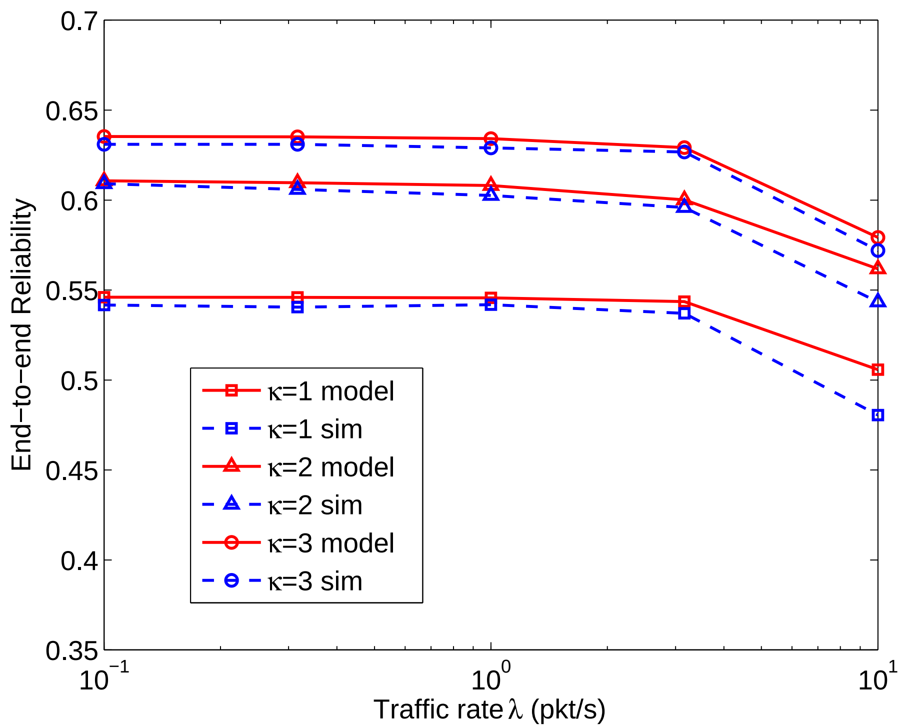

Fig. 17. End-to-end reliability vs. traffic rate λ for the multi-hop topology in Fig. 1c) with $a = -76$ dB, $b = 6$ dB, $\sigma = 6$.

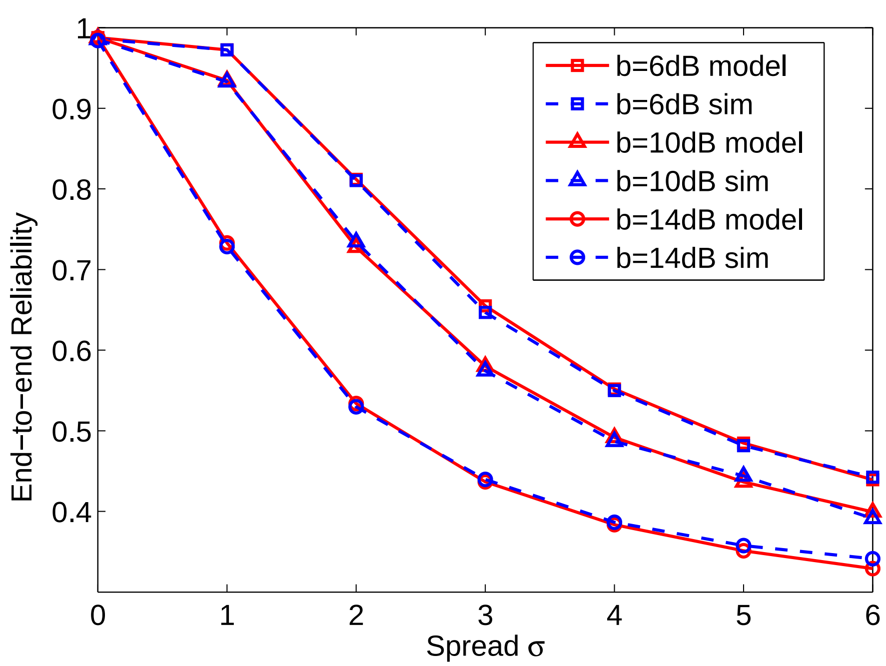

Fig. 18. End-to-end reliability vs. σ for the multi-hop topology in Fig. 1c) with $\lambda = 2$ pkt/s, $a = -76$ dB.